Techniques for Predicting Exposures to Polycyclic Aromatic Hydrocarbons (PAHs) Emitted from Cooking Processes for Cooking Workers

Chun-Yu Chen[1], Yu-Chieh Kuo[1], Shih-Min Wang[2], Kua-Rong Wu[1], Yu-Cheng Chen[3], Perng-Jy Tsai[1*]

[1] *Department of Environmental and Occupational Health, College of Medicine, National Cheng Kung University, Tainan 70403, Taiwan*
[2] *Department of Safety, Health and Environmental Engineering, Ming Chi University of Technology, New Taipei 24301, Taiwan*
[3] *National Environmental Health Research Center, National Health Research Institutes, Miaoli 35053, Taiwan*

ABSTRACT

Cooking oil fumes contain polycyclic aromatic hydrocarbons (PAHs), which are known to cause chronic human health effects; hence long-term exposure data is required for determining workers' exposure profiles and the resultant health risks. However, due to both time and cost constraints, previous studies were performed on a cross-sectional basis. To date, mathematical models have been widely used for predicting long-term exposures in the industrial hygiene field. The aims of this study were to develop suitable predictive models for establishing long-term exposure data on cooking workers. The whole study was conducted in a test chamber with an exhaust hood installed 0.7 m above a deep-frying pan and operated at flow rates of 2.64–5.16 m^3 min^{-1}. The cooking process that we selected for testing used peanut oil to deep-fry chicken nuggets at 200°C. An IOM inhalable sampler and an XAD-2 tube were successively used to collect particle- and gas-phase PAHs, respectively. All of the collected samples were analyzed for 21 PAHs using a gas chromatograph (GC) with tandem mass spectrometry (MS/MS). The results showed that the emission rates of the total-PAHs in the gas-phase and the particle-phase were 1.45×10^4 and 2.14×10^2 ng min^{-1}, respectively. The capture efficiencies of the exhaust hood for the total-PAHs were 39.1–76.5%. The resultant fugitive emission rates of the gas-phase and the particle-phase ranged from 3.41×10^3 to 8.82×10^3 and from 5.03×10^1 to 1.30×10^2 ng min^{-1}, respectively. As no significant difference in the sampling results of the total-PAHs was detected between the chef-zone (i.e., the near zone) and the helper-zone (i.e., the far zone), the well-mixed room (WMR) model was adopted for estimating the exposures of all workers. A good correlation (y = 0.134x + 75.3; R^2 = 0.860) was found between the model predicted results (x; 3.25×10^2–1.57×10^3 ng min^{-1}) and the field sampling results (y; 1.36×10^2–2.92×10^2 ng min^{-1}), indicating the plausibility of using the proposed approach to establish a long-term exposure databank for the cooking industry.

Keywords: Cooking fumes; Polycyclic aromatic hydrocarbons; Exposure assessment; Model prediction.

INTRODUCTION

Cooking fumes are known as one of the most significant indoor air pollution sources containing complex chemical compounds, including particulate matter, volatile organic compounds (VOCs), aromatic amines, polycyclic aromatic hydrocarbons (PAHs), etc. (Abdullahi *et al.*, 2013). Many studies have been conducted to investigate the emission rate of cooking-generated particles (Gao *et al.*, 2013), emissions of particles from cooking exhaust (Mi *et al.*, 2014), and chemical characteristics of particles of various cooking styles (Wang *et al.*, 2015). For PAH emissions from cooking sources, previous studies indicate that they could be emitted into the workplace environment when the cooking oil was heated between 180 and 270°C (Siegmann and Sattler, 1996; Zhu and Wang, 2003; Purcaro *et al.*, 2006). Cooking methods involved in the use of the cooking oil, such as stir-frying, pan-frying and deep-frying, generated more PAHs than those of water, such as boiling and steaming. In particular, the deep-frying process usually produces the highest PAHs as in comparison with other cooking methods (See and Balasubramanian, 2006, 2008), Chinese cooking methods generate higher levels of benzo[*a*]pyrene than that of the Western and Japanese restaurant (Li *et al.*, 2003), and five- and six-ringed PAHs were predominant in the composition of particles emitted from night market sources (Zhang *et al.*, 2015). PAH compounds such as benzo[*a*]pyrene has been

---

* Corresponding author.
  E-mail address: pjtsai@mail.ncku.edu.tw

proved to be carcinogenic (Culp *et al.*, 1998), and high-temperature frying oil fume has been classified into Group 2A (IARC, 2010).

Previous PAH exposure studies indicated that the naphthalene was the dominant compound (the breathing zone exposure concentrations = 0.15–0.27 µg m^{-3}) during the beefsteak pan-frying process (Sjaastad *et al.*, 2010). Benzo[*a*]pyrene concentrations fell to the range of 6–24 ng m^{-3} and 150–440 ng m^{-3} for home and commercial kitchens, respectively (Zhu and Wang, 2003). Although many PAH exposure assessment studies have been conducted, most of them were on the cross-sectional basis due to the cost constraints in both samplings and sample analyses. However, considering the chronic health effect of PAHs, the establishment of a long-term exposure data bank is needed for conducting exposure and health risk assessments.

To date, mathematical models have been widely used for predicting pollutant concentrations in the industrial hygiene field, particularly both the well-mixed room model and near-field (NF)/far-field (FF) model have been used in indoor environments with known dimensions, ventilation rates, and pollutant generation rates. For example, Nicas *et al.* (2006) used the near-field/far-field model to estimate benzene exposures, and a high R^2 (0.94) was obtained for predicting exposure of both fields. Gaffney *et al.* (2008) used both well-mixed room model and near-field/far-field model to estimate methanol exposure concentrations in a semiconductor manufacturing setting, better predictions were obtained from the latter than the former. In principle, if modeling results and measured concentrations had a good correlation, then obtaining a large amount of long-term exposure data might become possible even without conducting field measurements (AIHA, 2009; Kim *et al.*, 2009).

For cooking processes, both the well-mixed room model and near-field/far-field model have never been used for predicting workers' PAH exposures. Though workplace dimensions are usually available, the generated cooking fumes are known inherent with upward thermal drafting forces which might lead to the stratification of pollutant concentrations at different heights (Li and Delsante, 1996). In addition, considering the installation of ventilation (i.e., the exhaust hood), cooking fume emission rates should be replaced by the fugitive emission rates (i.e., should take the capture efficiencies of the exhaust hood into account) before model predictions. Therefore, the feasibility of using both the well-mixed room model and near-field/far-field model for predicting exposures of PAHs emitted from cooking processes requires further investigation.

The present study was conducted in a test room installed with a deep-frying apparatus and an exhaust hood with adjustable ventilation rate for a fixed cooking process (temperature and time, etc.). Emission rates of PAHs were measured, hood capture efficiencies were calculated, and resultant fugitive emission rates were estimated. Concentrations obtained from both the well-mixed room model and near-field/far-field model were predicted and compared with the measured values. Finally, the feasibilities of both models were assessed, and techniques for predicting

exposures of PAHs emitted from cooking processes were proposed. The results obtained from the present study would be helpful for cooking industries to establish long-term PAH exposure data for conducting exposure and health risk assessments.

MATERIALS AND METHODS

Test Room and Test Cooking Condition

All experiments were conducted in a test room (L × W × H = 3.25 m × 3.10 m × 2.75 m) with a general kitchen settings (Chiang *et al.*, 1998) including an electronic deep-frying machine (2000 W, L × W = 30 cm × 15.3 cm; WFT-4L, WISE Inc., Taipei, Taiwan) with a cooking surface 1.1 m above the floor, and a kitchen exhaust hood (L × W = 89 cm × 52 cm; DR-7790ASXL, Sakura Corp., Taichung, Taiwan) placed at 0.7 m above from the deep-frying machine (i.e., 1.8 m above the floor). For each deep-frying test run, it contains 9 repeated cycles, and each cycle includes a 5-min deep-frying period, and followed by a 5-min rest (i.e., the whole test run lasts for 90 minutes). During each deep-frying period, 300 g fresh chicken nuggets were deep-fried at 200°C in 3 L peanut oil. The cooking oil was repeated used for the whole test run. Three default flow rates of the exhaust hood (i.e., low, medium, and high = 2.64, 3.69, and 5.16 m^3 min^{-1}, respectively) were selected in the present study. The only door and window of the test room were closed during the experiment period.

Sampling for PAH Emission Rates and Exposure Concentrations

For each selected ventilation rate, three test runs were conducted to determine its PAH emission rate (G) and resultant exposure concentrations inside the test room. For sampling the emission rate, the test system (including the electronic deep-frying machine and the exhaust hood) was enclosed completely to ensure the non-releasing of emitted PAHs, and a sampling train was placed 15 cm beneath the exhaust hood (Fig. 1), which includes an IOM personal inhalable sampler (Cat. No. 225-70A, SKC Inc., MN, USA) with a quartz fiber filter for collecting particle-phase PAHs, and followed by an XAD-2 tube (Amberlite$^®$ XAD$^®$-2, Sigma-Aldrich Corp., MO, USA) for collecting gas-phase PAHs.

Exposure concentrations of PAHs inside the test room were measured using the same sampling train but placed on a mannequin. Samples were collected from both sites of the chef-zone (CZ) (1.5 m in height above the floor, and 0.5 m away from the deep-frying machine to represent the exposure of chefs), and the helper-zone (HZ) (1.5 m in height above the floor, and 1.5 m away from the deep-frying machine to represent the exposures of chefs' helpers) (Fig. 2).

PAH Analysis

In the present study, each collected filter was microwave extracted using a mixed solvent (*n*-hexane and dichloromethane, V:V = 1:1, 25 mL) for 1 hr. For each collected XAD-2 sample, it was extracted using ultrasonic
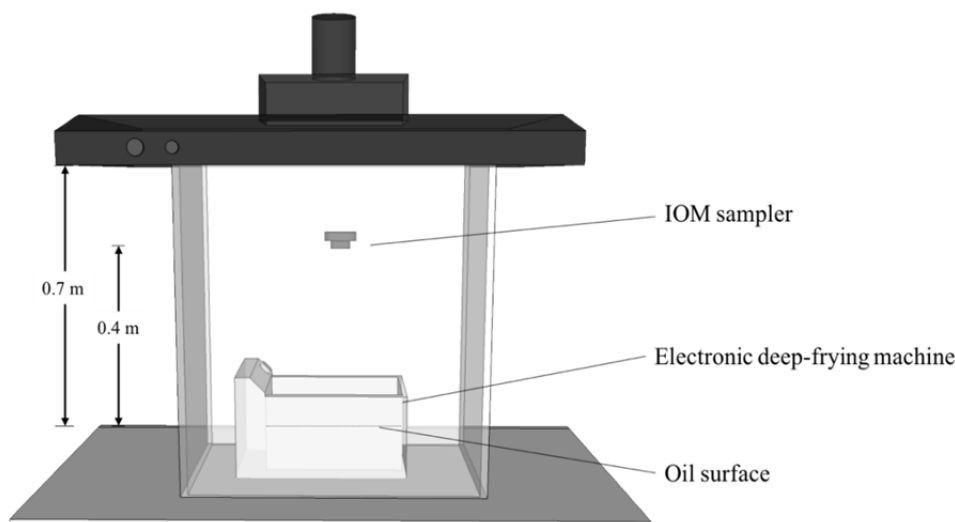
Fig. 1. Schematic of the site for placing IOM sampler for determining PAH emission rates when the exhaust hood and deep frying machine are in an enclosure condition.

bath with 2 mL dichloromethane (DCM) for 1 hr (one cycle for 15-min ultrasonic bath followed by 5-min rest, and repeated continuously for three cycles). The extracted samples were then concentrated to ~5 mL, and cleaned up using the YMC silica gel tube (NH$_2$ 12 g, 50 µm; YMC-DispoPackAT, YMC Co., Ltd., Kyoto, Japan) to ensure no oil was present in the samples. Then, the above samples were re-concentrated and diluted to exactly 1.0 mL. The PAH content was determined using a gas chromatograph (GC) (Agilent 7890B, Agilent Technologies Inc., CA, USA) with tandem mass spectrometry (MS/MS) (Agilent 7000C MS/MS Triple Quad, Agilent Technologies Inc., CA, USA) and a computer workstation. This GC/MS/MS was equipped with an Agilent 122-9632 DB-EUPAH column (30 m [length] × 0.32 mm [I.D.], film thickness = 0.25 µm) (Agilent 122-9632 DB-EUPAH, Agilent Technologies Inc., CA, USA) and an Agilent 7693 automatic sampler (Agilent 7693, Agilent Technologies Inc., CA, USA) and was operated under the following conditions: injection volume 10 µL; splitless injection at 310°C; ion sources temperature at 310°C; and oven from 80°C to 200°C at 20°C min^{-1}, 200°C to 355°C at 8°C min^{-1}, hold at 355°C for 17.325 min. The masses of primary and secondary ions of PAHs were determined with the scan mode for pure PAH standards. Qualification of PAHs was performed using the selected ion monitoring (SIM) mode.

The concentrations of 21 PAH species were determined, including naphthalene (Nap), acenaphthylene (AcPy), acenaphthene (Acp), fluorene (Flu), phenanthrene (PA), anthracene (Ant), fluoranthene (FL), pyearene (Pyear), cyclopenta[*c,d*]pyearene (CYC), benzo[*a*]anthracene (BaA), chrysene (CHR), benzo[*b*]fluoranthene (BbF), benzo[*k*]fluoranthene (BkF), benzo[*e*]pyearene (BeP), benzo[*a*]pyearene (BaP), perylene (PER), indeno[1,2,3-*cd*]pyearene (IND), dibenzo[*a,h*]anthracene (DBA), benzo[*b*]chrycene (BbC), benzo[*ghi*]perylene (BghiP), and coronene (COR). The GC/MS/MS was calibrated with a diluted standard solution of 16 PAH compounds (PAH Mixture-610M, Supleco) plus 5 additional individual PAHs obtained from Merck. Analysis of serial dilutions of PAH standards showed the detection limit of GC/MS/MS falling to the range from 0.06 to 0.45 ppb for the analyzed 21 PAH compounds. Ten consecutive injections of a PAH 610-M standard yielded an average relative standard deviation (RSD) of GC/MS integration area of 3.0% with a range of 0.8–5.1%. Quality control (QC) samples adopted the median level of the low calibration curve (30 ppb), and were analyzed along with each batch. The QC results were required to fall within ± 20% of the calibration curve. To evaluate analytical precision, one spike sample and one random replicate sample were analyzed for each batch. Recovery efficiencies were determined using a solution containing known PAH concentrations following the same experimental procedures used for the treatment of samples. This study showed recovery efficiencies for the 21 PAH compounds ranging from 65.0% to 117.5%, with an average value of 90.9%. Analysis of field blanks and method blanks, including the glass fiber filter and XAD-2 cartridge, found no significant contamination (GC/MS/MS integrated area < detection limit).

Data Analysis

In this study, the total-PAH concentration were regarded as the sum of the concentrations of 21 PAH compounds for each collected sample. In order to assess the PAH homolog distribution for each collected sample, the total-PAH were further classified into three categories, including the low molecular weight PAHs (LMW-PAHs, containing 2- to 3-ringed PAHs), middle molecular weight PAHs (MMW-PAHs, containing 4-ringed PAHs), and high molecular weight PAHs (HMW-PAHs, containing 5- to 7-ringed PAHs). Moreover, considering that several PAH compounds have been found to be human carcinogens, the carcinogenic potencies associated with PAHs emissions from each emission source were also determined. In principle, the carcinogenic potency of a given PAH compound can be assessed based on its
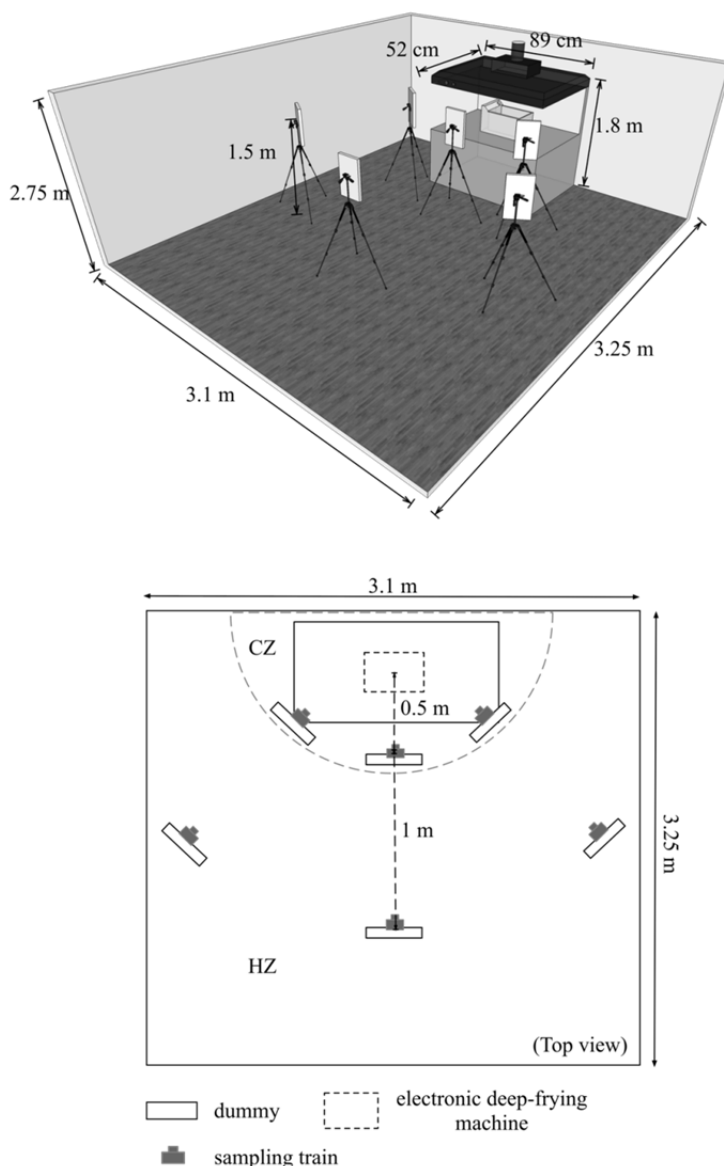
Fig. 2. Schematic of sites for collecting near-field and far-field PAH exposure concentrations.

benzo[*a*]pyearene equivalent concentration (i.e., BaP$_{eq}$). Calculation of the BaP$_{eq}$ concentration for a given PAH compound requires the use of the toxic equivalent factor (TEF), which represents the relative carcinogenic potency of the given PAH compound by reference to the specific compound BaP, to adjust its original concentration. To date, several proposals for TEFs (Nisbet and LaGoy, 1992; Malcolm and Dobson, 1994; Larsen and Larsen, 1998) are used in the present study (Table 1). On the basis of this TEF list, the carcinogenic potency of the total-PAHs (i.e., the total-BaP$_{eq}$) could be assessed using Eq. (1):

$$Total - BaP_{eq} = \sum_{i=1}^{21} PAH_i \times TEF_i \;.$$
(1)

where PAH_i and TEF_i are the concentration of the ith PAH compound and its TEF, respectively.

Determining Capture Efficiencies of the Exhaust Hood and Fugitive Emission Rates

For the purpose of estimating exposures of cooking workers, PAH emission rates (G) of the investigated cooking process should be replaced by the fugitive emission rates (ER$_f$). Assuming the capture efficiencies (ε; %) of the exhaust hood is known, then ER$_f$ can be obtained using the following equation:

$$ER_f = G \times ((100 - \varepsilon)\%$$
(2)

In principle, the high temperature will lead to a thermal draft with an upward air current during cooking processes. As the heated air rises, it mixes turbulently with the surrounding air. This results in an increasing air plume diameter and volumetric flow rates. The plume flow rate of the thermal draft at the hood entry level can be estimated as the following equation (Popiołek *et al.*, 1998):

Table 1. The studied 21 PAH compounds and their TEFs proposed by Larsen and Larsen (1998), Malcolm and Dobson (1994), Nisbet and LaGoy (1992), and those adopted in the present study.

PAHs	(Larsen and Larsen, 1998)	(Malcolm and Dobson, 1994)	(Nisbet and LaGoy, 1992)	This study
NaP	-	0.001	0.001	0.001
AcPy	-	0.001	0.001	0.001
Acp	-	0.001	0.001	0.001
Flu	0.05	0.001	0.001	0.05
PA	0.0005	0.001	0.001	0.001
Ant	0.0005	0.01	0.01	0.01
FL	-	0.001	0.001	0.001
Pyr	0.001	0.001	0.001	0.001
BaA	0.005	0.1	0.1	0.1
CHR	0.03	0.01	0.01	0.03
CYC	0.02	0.1	-	0.1
BbF	0.1	0.1	0.1	0.1
BkF	0.1	0.1	0.1	0.1
BeP	0.002	0.001	-	0.002
BaP	1	1	1	1
PER	-	0.001	-	0.001
DBA	1	1	1	1
IND	-	0.1	0.1	0.1
BbC	-	-	-	-[a]
BghiP	0.02	0.01	0.01	0.02
COR	-	0.001	-	0.001

[a] No TEF has been suggested.

$$Q_p = K_v E^{1/3}(h + Z)^{5/3} \tag{3}$$

where Q_p is the plume flow rate at the hood entry level ($m^3\ s^{-1}$), E is the heat source power (W), h is the height from the heat source to the hood entry (m), Z is the distance between the heat source and the origin point of the plume (m), and K_v is the coefficient describing the air entrainment by the plume. Here, K_v and Z were as suggested by Yik and Au (2002) to be 0.0065 and 2.25 D for cooking processes, respectively. The capture efficiency (ε) of gaseous pollutants emitted from the cooking process can be determined using Eq. (4):

$$\varepsilon = \frac{q_f}{Q_p} \times 100\% = \frac{q_f}{0.0065E^{1/3}\left(H+2.25D\right)^{5/3}} \times 100\%, \tag{4}$$

if $q_f > Q_p$, $\varepsilon = 100\%$,

where q_f is the exhaust flow rate ($m^3\ s^{-1}$). Considering particle phase pollutants emitted from the cooking process were dominated by PM_1 (Lunden *et al.*, 2015), which suggests that their capture efficiencies could also be adopted for gas phase pollutants (i.e., Eq. (4)). Therefore, Eq. (4) was adopted for determining the capture efficiencies (ε) for the total-PAHs, gas-phase PAHs, particle-phase PAHs, and total-BaP_{eq} in the present study.

The Selected Prediction Models

In the present study, both the well-mixed room model and near-field/far-field model were selected for predicting workers' PAH exposures. Firstly, we assume that fugitive emissions will be mixed completely in the kitchen space

instantly due to the limited kitchen space and strong mixing effect. Therefore, the obtained fugitive emission rates of PAHs (ER_f) were applied to the well-mixed room model (Reinke and Keil, 2006) to predict the exposures of all workers in the test room (i.e., including chefs and their helpers, and assuming both share the same exposure level) using Eq. (5):

$$C_{WMR} = \left(C_0 - C_{in} - \frac{ER_f}{Q}\right)e^{\frac{-Q(t-t_0)}{V}} + C_{in} + \frac{ER_f}{Q} \tag{5}$$

where C_{WMR} is the concentration predicted for all workers at time t, C_0 is the concentration of test room at time t_0, C_{in} is the concentration of the inlet air, Q is the inlet air flow rate, and V is the volume of the test room. Secondly, we assume that fugitive emissions will affect more strongly on the exposure of workers who are closer than those of less close to the emission source. In this situation, the obtained fugitive emission rates of PAHs (ER_f) were also applied to the near-field/far-field model (Nicas, 2006) to estimate the exposures of chefs (i.e., near-field exposures) and their helpers (i.e., far-field exposures) using Eqs. (6) and (7), respectively:

$$sC_{NF} = \frac{ER_f}{Q} + \frac{ER_f}{\beta} + ER_f\left(\frac{\beta \cdot Q + \lambda_2 \cdot V_N\left(\beta+Q\right)}{\beta \cdot Q \cdot V_N\left(\lambda_1 + \lambda_2\right)}\right)e^{\lambda_1 \cdot t}$$
$$- ER_f\left(\frac{\beta \cdot Q + \lambda_1 \cdot V_N\left(\beta+Q\right)}{\beta \cdot Q \cdot V_N\left(\lambda_1 - \lambda_2\right)}\right)e^{\lambda_2 \cdot t}, \tag{6}$$

$$C_{FF} = \frac{ER_f}{Q}$$

$$+ER_f \left(\frac{\lambda_1 \cdot V_N + \beta}{\beta} \right) \left(\frac{\beta \cdot Q + \lambda_2 \cdot V_N (\beta + Q)}{\beta \cdot Q \cdot V_N (\lambda_1 - \lambda_2)} \right) e^{\lambda_1 \cdot t} \quad (7)$$

$$-ER_f \left(\frac{\lambda_2 \cdot V_N + \beta}{\beta} \right) \left(\frac{\beta \cdot Q + \lambda_1 \cdot V_N (\beta + Q)}{\beta \cdot Q \cdot V_N (\lambda_1 - \lambda_2)} \right) e^{\lambda_2 \cdot t},$$

where C_{NF} and C_{FF} are the concentrations predicted respectively for chefs and helpers at time t, V_N and V_F are respectively as the volume of near-field and far-field, β is the air exchange rate between near-field and far-field, and λ_1 and λ_2 respectively represent the air turnover rates of near-field and far-field (in min^{-1}).

RESULTS AND DISCUSSION

PAH Emission Rates

Table 2 shows the emission rates (or the generation rates) of the gas-phase PAHs, particle-phase PAHs, LMW-PAH, MMW-PAH, HMW-PAH and total-BaP$_{eq}$ for the test cooking conditions. Results show that emission rates of the gas-phase PAHs and particle-phase PAHs were 1.45×10^4 ng min^{-1} and 2.14×10^2 ng min^{-1}, respectively. Most

generated PAHs were in the form of the gas-phase (98.5%) and were mainly contributed by LMW-PAHs (i.e., PAHs with 2–3 benzene rings). It is known that PAHs can be generated from cooking processes because of the incomplete combustion or pyrolysis of organic compounds containing hydrogen and carbon. Since temperatures involved in the selected cooking processes is quite low (i.e., 200°C) which can only provide very limited power for the formation of PAHs, it is not so surprising to see the dominance of LMW-PAHs (especially naphthalene) in the emitted PAHs. The above inference can also be supported by many cooking-related studies (Schauer *et al.*, 1999, 2002; McDonald *et al.*, 2003; Sjaastad *et al.*, 2010). However, the naphthalene emission rates of the above studies (range = 127–588 µg min^{-1}) were much higher than those found in the present study due to the involved cooking food weights for those of formers (12.5–68 kg) was much higher than that of the latter (2.7 kg). The above inference can be further supported by the comparable emission factors obtained from those of the formers (4.5–16.7 µg min^{-1} kg^{-1}) and the latter (5.4 µg min^{-1} kg^{-1}).

For particle-phase PAHs, the emission rates of LMW-, MMW-, and HMW-PAHs were 8.97×10^1, 1.14×10^2, 1.00×10^1 ng min^{-1}, respectively. PAHs with 3–4 benzene rings (i.e., MMW-PAHs) were found to be the most dominant

Table 2. PAHs emission rates of the gas-phase and particle phase (n = 6).

PAHs species	Gas-phase			Particle-phase		
	Mean (ng min^{-1})	SD (ng min^{-1})	Percentage	Mean (ng min^{-1})	SD (ng min^{-1})	Percentage
Naphthalene	1.12×10^4	6.68×10^2	77.17%	5.10	1.41	2.38%
Acenapthylene	2.08×10^3	3.68×10^2	14.38%	3.28	9.30×10^{-1}	1.54%
Acenapthene	1.02×10^2	2.08×10^1	0.71%	8.30×10^{-1}	1.70×10^{-1}	0.39%
Fluorene	3.36×10^2	6.50×10^1	2.32%	7.10×10^{-1}	4.20×10^{-1}	0.33%
Phenanthrene	4.88×10^2	9.03×10^1	3.37%	4.62×10^1	1.13×10^1	21.62%
Anthracene	2.98×10^2	6.20×10^1	2.06%	3.35×10^1	7.49	15.68%
Fluoranthene	ND	--	--	5.77×10^1	1.18×10^1	27.00%
Pyrene	ND	--	--	4.76×10^1	1.01×10^1	22.24%
Benzo(a)anthracene	ND	--	--	4.17	8.30×10^{-1}	1.95%
Chrysene	ND	--	--	4.68	9.40×10^{-1}	2.19%
Cyclopenta(c,d)pyrene	ND	--	--	4.25	1.00	1.99%
Benzo(b)fluoranthrene	ND	--	--	1.26	2.60×10^{-1}	0.59%
Benzo(k)fluoranthrene	ND	--	--	8.40×10^{-1}	1.70×10^{-1}	0.39%
Benzo(e)pyrene	ND	--	--	1.02	2.50×10^{-1}	0.48%
Benzo(a)pyrene	ND	--	--	1.76	5.00×10^{-1}	0.82%
Perylene	ND	--	--	ND	--	--
Dibenz(a,h)anthracene	ND	--	--	ND	--	--
Indeno(1,2,3,-cd)pyrene	ND	--	--	ND	--	--
Benzo(b)chrysene	ND	--	--	ND	--	--
Benzo(g,h,i)perylene	ND	--	--	8.90×10^{-1}	1.80×10^{-1}	0.42%
Coronene	ND	--	--	ND	--	--
LMW-PAHs	1.45×10^4	9.24×10^1	100%	8.97×10^1	1.80×10^1	41.94%
MMW-PAHs	ND	--	--	1.14×10^2	2.35×10^1	53.38%
HMW-PAHs	ND	--	--	1.00×10^1	2.29	4.68%
Total-PAHs	1.45×10^4	1.03×10^3	98.55%	2.14×10^2	4.35×10^1	1.45%
Total-BaP$_{eq}$	3.36×10^1	5.02	90.53%	3.52	8.90×10^{-1}	9.47%

ND: non-detected.

compounds, which accounted for 53.38% of particle-phase PAHs. Similar results can also be found in other studies (Rogge *et al.*, 1991; McDonald *et al.*, 2003; Saito *et al.*, 2014). They found that particle-phase PAHs contain mainly 3–4 ringed compounds, and the two compounds of fluoranthene (FL) and pyrene (Pyr) were found with the highest fractions.

Although particle-phase PAHs accounted for only 1.5% of the total-PAH emissions, a higher contribution (9.5%) to the total-BaP$_{eq}$ emission rates was found in the present study. The above result is not so surprising because MMW- and HMW-PAHs are the most dominant compounds in particle-phase PAHs, and which compounds are known with higher TEFs.

Capture Efficiency and Fugitive Emission Rates

For the purpose of estimating cooks' exposures, PAH emission rates (or generation rates; G) should be replaced by fugitive emission rates (ER_f). Therefore, the estimation of hood capture efficiencies (ε) become essential to meet the above purpose. In the present study, the heat source power (E), exhaust flow rate (q_f), exhaust hood height (H), and diameter of the heat source (D, using equivalent surface diameter) were found to be 0.7 m, 2000 W, and 0.242 m, respectively. Based on Eq. (4), the capture efficiencies (ε) of the exhaust hood were found to be 39.1%, 54.7%, and 76.5% for three designated exhaust flow rates of 2.64, 3.69, and 5.16 m³ min⁻¹, respectively. The above captured efficiencies were quite comparable to those obtained from Yik and Au (2002) (i.e., 39100%).

The obtained capture efficiencies, together with the obtained emission rates (G) (Table 2) can be used to estimate the fugitive emission rates (ER_f) using Eq. (2). The resultant ER_f values for the exhaust flow rates (Q) set at 2.64, 3.69, and 5.16 m³ min⁻¹ for the total-PAHs were found to be 8.95 × 10³, 6.66 × 10³, and 3.46 × 10³ ng min⁻¹, respectively; those for the gas-phase PAHs were 8.82 × 10³, 6.57 × 10³, and 3.41 × 10³ ng min⁻¹, respectively; those for the particle-phase PAHs were 1.30 × 10², 9.69 × 10¹, and 5.03 × 10¹ ng min⁻¹, respectively; and those for the total-BaP$_{eq}$ were 2.26 × 10¹, 1.68 × 10¹, and 8.70 ng min⁻¹, respectively. The above results were not so surprising since the increase in the exhaust flow rates (Q) would result in the increase in the capture efficiencies (ε), which leads to the decrease in the fugitive emission rates (ER_f).

Predicted PAH Exposure Concentrations

Table 3 shows the predicted PAH exposure concentrations (including the gas-phase PAHs, particle-phase PAHs, LMW-PAH, MMW-PAH, HMW-PAH and total-BaP$_{eq}$) for all workers (i.e., C_{WMR} representing predicted PAH exposure concentrations for workers in both NF and FF), chefs' exposure concentrations (i.e., C_{NF} representing the predicted concentrations for workers in the NF), and helpers' exposure concentrations (i.e., C_{FF} representing the predicted concentrations for workers in the FF) under three designated exhaust hood flow rates (i.e., 2.64 m³ min⁻¹, 3.69 m³ min⁻¹, and 5.16 m³ min⁻¹) using Eqs. (5), (6), and (7), respectively. The average random airspeed (β) used in the NF/FF model

Table 3. Predicted NF, FF and WMR concentrations (C_{NF}, C_{FF}, and C_{WMR}) of PAHs for the exhaust hood operated under three designated flow rates (Q).

PAHs concentrations (ng m⁻³)	Hood exhaust flow rate (Q, m³ min⁻¹)								
	2.64			3.69			5.16		
	C_{NF}	C_{FF}	C_{WMR}	C_{NF}	C_{FF}	C_{WMR}	C_{NF}	C_{FF}	C_{WMR}
Gas-phase	2.27 × 10³	1.50 × 10³	1.53 × 10³	1.40 × 10³	8.26 × 10²	8.43 × 10²	5.39 × 10²	3.14 × 10²	3.20 × 10²
Particle-phase	3.35 × 10¹	2.21 × 10¹	2.26 × 10¹	2.07 × 10¹	1.22 × 10¹	1.24 × 10¹	7.95	4.63	4.73
Total-PAHs	2.33 × 10³	1.54 × 10³	1.57 × 10³	1.43 × 10³	8.44 × 10²	8.55 × 10²	5.47 × 10²	3.19 × 10²	3.25 × 10²
Total-BaP$_{eq}$	5.83	3.85	3.92	3.60	2.12	2.16	1.38	8.10 × 10⁻¹	8.20 × 10⁻¹

was measured using an anemometer (TSI 9565-X, TSI Inc., MN, USA) with a thermo-anemometer probe (TSI 966, TSI Inc., MN, USA). In the present study, β was 0.03, 0.03, and 0.04 m s^{-1} when the exhaust hood flow rates were set at 2.64, 3.69, and 5.16 m^3 min^{-1}, respectively. Results show that PAH concentrations (including the gas-phase PAHs, particle-phase PAHs, LMW-PAH, MMW-PAH, HMW-PAH and total-BaP$_{eq}$) in magnitude for the three predicted results were: $C_{NF} > C_{WMR} > C_{FF}$ (Table 3). Since workers in the NF were closer to the emission source than those in FF, the predicted PAH exposure concentrations of C_{NF} and hence were higher than that of C_{FF}. On the other hand, C_{WMR} represents the emitted PAHs being uniformly distributed in the test room, and hence it can be expected that the magnitudes of C_{WMR} fall between C_{NF} and C_{FF}.

Measured PAH Exposure Concentrations

Table 4 shows the measured PAH exposure concentrations for all workers (i.e., C_T, including sampling results obtained from both chef-zone (CZ) and helper-zone (HZ)), chef exposure concentrations (i.e., C_{CZ}, sampling results obtained from CZ) and helper exposure concentrations (i.e., C_{HZ}, sampling results obtained from HZ) under three designated exhaust hood flow rate conditions (i.e., 2.64 m^3 min^{-1}, 3.69 m^3 min^{-1}, 5.16 m^3 min^{-1}). Results show that LMW-PAHs dominated in all the measured total-PAH concentrations, including C_T, C_{CZ} and C_{HZ}. The above results were consistent with that of fugitive PAH emission results. In particular, most of the total PAH concentration was contributed by the naphthalene (~90%), which was also consistent with the results reported by Sjaastad *et al.* (2010). Though the measured PAH concentrations for C_{CZ} were slightly higher than that of C_{HZ}, but no significant difference could be found in the present study (P > 0.05). Therefore, workers in the test kitchen may have very similar PAH exposures regardless of their locations. This could be explained by the circulation of airflow in the test room. In principle, cooking oil fumes could be first lifted by the thermal draft, then partly removed by the exhaust hood, and the rest reach the ceiling of the kitchen, then turn downward to the floor, and finally combine with the new generated cooking oil fumes, and then repeat the above cycle. As a result, a well-mixed condition was found in the test room which leads to no significant difference in PAH concentration between C_{CZ} and C_{HZ}.

Considering there was no significant difference between the C_{CZ} and C_{HZ}, both results were combined to describe the overall PAH concentrations (C_T) in the test room. For C_T, Table 4 also shows that the mean total-PAHs were increased from 1.36 × 10^2 to 2.93 × 10^2 ng m^{-3} as exhaust hood flow rates decreased from 5.16 m^3 min^{-1} to 2.64 m^3 min^{-1}. Obviously, the above results can be explained by the fact that the increase in the exhaust hood flow rates would result in the increases in the capture efficiencies.

Table 4 also shows that all measured PAH exposure concentrations (i.e., C_{CZ}, C_{HZ}, and C_T) were ~5 times in magnitude less than the corresponding predicted exposure concentrations (i.e., C_{NF}, C_{FF}, and C_{WMR}). Here, it should be noted that the predictions of C_{NF}, C_{FF}, and C_{WMR} assumes well-mixed PAH concentrations in the designated zones. However, the thermal draft effect would result in higher concentrations accumulated at the ceiling, and decreased as the height decreased. The above inference is supported by our findings (i.e., C_{CZ}, C_{HZ}, and C_T were much lower than that of the corresponding C_{NF}, C_{FF}, and C_{WMR}). In addition, the stratified concentration scenario also suggests the concentrations at the same height could be very similar. Since C_{CZ}, C_{HZ}, and C_T were measured at the same height (i.e., 1.5 m in height from the floor), no significant difference in their measured results could be theoretically plausible.

Table 4. Measured chef, helper and all worker concentrations (C_{CZ}, C_{HZ}, and C_T) of PAHs for the exhaust hood operated under three designated flow rates (Q).

Hood exhaust flow rate (Q, m^3 min^{-1})	PAHs concentrations (ng m^{-3})	LMW-PAHs	MMW-PAHs	HMW-PAHs	Total-PAHs	Total-BaP$_{eq}$
2.64 (n = 3)	C_{CZ}	2.92 × 10^2	1.97	9.65 × 10^{-1}	2.95 × 10^2	7.90 × 10^{-1}
	SD	1.42 × 10^1	8.80 × 10^{-1}	4.30 × 10^{-1}	1.45 × 10^1	1.10 × 10^{-1}
	C_{HZ}	2.89 × 10^2	1.25	6.75 × 10^{-1}	2.91 × 10^2	7.47 × 10^{-1}
	SD	3.08 × 10^1	5.20 × 10^{-1}	2.80 × 10^{-1}	3.11 × 10^1	9.00 × 10^{-2}
	C_T	2.90 × 10^2	1.61	8.20 × 10^{-1}	2.93 × 10^2	7.64 × 10^{-1}
	SD	2.11 × 10^1	6.20 × 10^{-1}	3.20 × 10^{-1}	2.11 × 10^1	9.00 × 10^{-2}
3.69 (n = 3)	C_{CZ}	1.61 × 10^2	8.03 × 10^{-1}	4.78 × 10^{-1}	1.62 × 10^2	5.20 × 10^{-1}
	SD	3.10 × 10^1	2.40 × 10^{-1}	1.40 × 10^{-1}	3.07 × 10^1	5.00 × 10^{-2}
	C_{HZ}	1.52 × 10^2	1.04	5.34 × 10^{-1}	1.54 × 10^2	5.87 × 10^{-1}
	SD	1.95 × 10^1	1.60 × 10^{-1}	8.00 × 10^{-2}	1.93 × 10^1	7.00 × 10^{-2}
	C_T	1.57 × 10^2	9.19 × 10^{-1}	5.06 × 10^{-1}	1.58 × 10^2	5.51 × 10^{-1}
	SD	2.53 × 10^1	2.00 × 10^{-1}	1.10 × 10^{-1}	2.50 × 10^1	5.00 × 10^{-2}
5.16 (n = 3)	C_{CZ}	1.40 × 10^2	7.28 × 10^{-1}	3.85 × 10^{-1}	1.41 × 10^2	3.59 × 10^{-1}
	SD	1.37 × 10^1	2.00 × 10^{-1}	1.10 × 10^{-1}	1.34 × 10^1	1.00 × 10^{-2}
	C_{HZ}	1.30 × 10^2	7.00 × 10^{-1}	3.54 × 10^{-1}	1.31 × 10^2	3.45 × 10^{-1}
	SD	2.53 × 10^1	2.40 × 10^{-1}	1.20 × 10^{-1}	2.56 × 10^1	1.20 × 10^{-1}
	C_T	1.35 × 10^2	7.14 × 10^{-1}	3.70 × 10^{-1}	1.36 × 10^2	3.52 × 10^{-1}
	SD	1.01 × 10^1	2.20 × 10^{-1}	1.10 × 10^{-1}	1.02 × 10^1	6.00 × 10^{-2}

Proposal for Predicting Workers' PAH Exposure Concentrations

Since the measured PAH concentrations of C_{CZ} and C_{HZ} were not significantly different, the WMR model was selected to serve as a basis for predicting the PAH exposure concentrations. Fig. 3 shows the relationship between WMR model predicted results (i.e., C_{WMR}) and field measured results (i.e., C_T) on the gas-phase PAHs, particle-phase PAHs, total-PAHs, and total-BaP_{eq} basis. High R^2 were consistently found in the gas-phase PAHs, particle-phase PAHs, total-PAHs, and total-BaP_{eq} (0.857, 0.711, 0.860, and 0.92, respectively). The above results suggest that the WMR model can be used as a basis for predicting the PAH exposure concentrations of cooking workers.

Comparable R^2 and regression equations were obtained for the gas-phase PAHs and total-PAHs, which obviously can be explained by the fact that the total-PAHs were dominated by gas-phase PAHs. The particle-phase PAHs were found with the lowest R^2, which indicated that the variation in the particle-phase PAHs was higher than that of others. The regression equation for the total-BaP_{eq} concentrations much comparable to that of particle-phase PAHs, rather than gas-phase PAHs. The above results can be explained by the high TEFs assigned for MMW-PAHs

and HMW-PAHs (i.e., main contributors in particle-phase PAHs), and variation of particle-phase PAH was mainly contributed by the LMW-PAHs.

Yet, it is true that the resultant regression equations might be not universally applicable. The approach proposed by the present study provides a possibility for establishing a long-term exposure databank for cooking industries for less constraints in both samplings and sample analyses.

CONCLUSIONS

Most of the generated PAHs were gaseous and low in molecular weight. Although particle-phase PAHs accounted for a very low fraction of the total-PAH emissions, they contributed a larger share to the total-BaP_{eq} emission rates in the present study. The capture efficiencies of the exhaust hood fell in the range of 39.1–76.5%, indicating that fugitive PAH emissions are theoretically plausible. All of the measured PAH exposure concentrations were ~5 times less in magnitude than the corresponding predicted exposure concentrations. Since C_{CZ}, C_{HZ}, and C_T were measured at the same height, the lack of a significant difference between their measured concentrations can be explained by the circulation effect. On the other hand, the values for
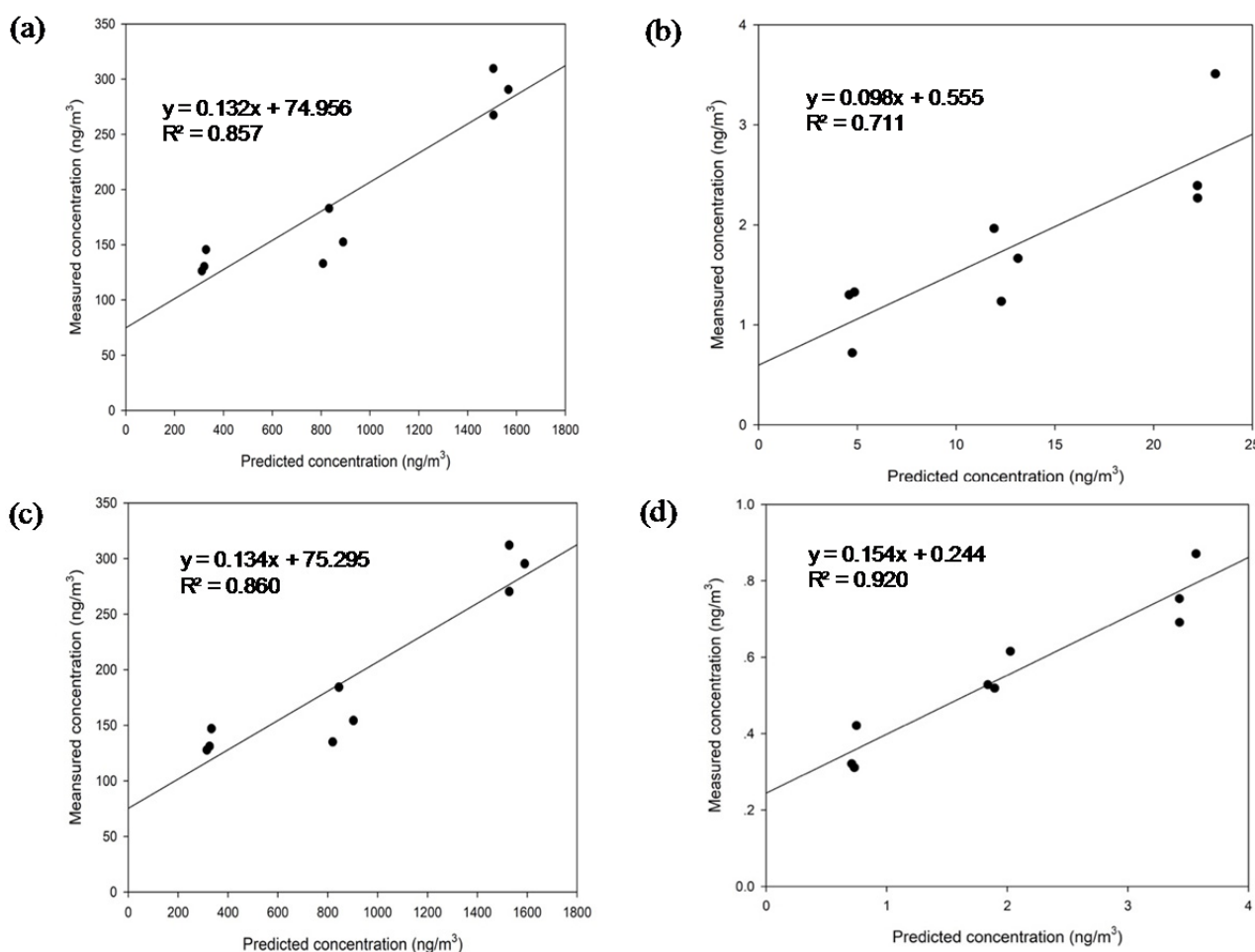
Fig. 3. Relationships between measured (y) and predicted (x) exposure concentrations for the (a) gas-phase PAHs, (b) particle-phase PAHs, (c) total-PAHs, and (d) total-BaP_{eq} (n = 9).

C_{CZ}, C_{HZ}, and C_T were much lower than those for C_{NF}, C_{FF}, and C_{WMR}, which suggests that the PAH concentrations might have been stratified in the atmosphere of the test room. The relationship between the WMR model predicted results and the field measured results exhibited a high R^2, indicating that the WMR model can serve as a reliable basis for predicting the PAH exposure concentrations of cooking workers. Although the resultant regression equations may not be universally applicable, the present study has proposed a suitable approach to establishing a long-term exposure databank for cooking industries with fewer constraints on both sampling and sample analysis.

ACKNOWLEDGMENT

REFERENCES

Abdullahi, K.L., Delgado-Saborit, J.M. and Harrison, R.M. (2013). Emissions and indoor concentrations of particulate matter and its specific chemical components from cooking: A review. *Atmos. Environ.* 71: 260–294.

AIHA (2009). *Mathematical models for estimating occupational exposure to chemicals, 2nd deition*. American Industrial Hygiene Association, Washington, USA.

Chiang, T.A., Wu, P.F. and Ko, Y.C. (1998). Prevention of exposure to mutagenic fumes produced by hot cooking oil in taiwanese kitchens. *Environ. Mol. Mutagen.* 31: 92–96.

Culp, S.J., Gaylor, D.W., Sheldon, W.G., Goldstein, L.S. and Beland, F.A. (1998). A comparison of the tumors induced by coal tar and benzo[a]pyrene in a 2-year bioassay. *Carcinogenesis* 19: 117–124.

Gaffney, S., Moody, E., McKinley, M., Knutsen, J., Madl, A. and Paustenbach, D. (2008). Worker exposure to methanol vapors during cleaning of semiconductor wafers in a manufacturing setting. *J. Occup. Environ. Hyg.* 5: 313–324.

Gao, J., Cao, C.S., Wang, L., Song, T.H., Zhou, X., Yang, J. and Zhang, X. (2013). Determination of size-dependent source emission rate of cooking-generated aerosol particles at the oilheating stage in an experimental kitchen. *Aerosol Air Qual. Res.* 13: 488–496.

IARC (2010). Household use of solid fuels and high-temperature frying, Cancer, International Agency for Research on Cancer, Lyon.

Kim, S.Y., Sheppard, L. and Kim, H. (2009). Health effects of long-term air pollution: Influence of exposure prediction methods. *Epidemiology* 20: 442–450.

Larsen, J.C. and Larsen, P.B. (1998). Chemical carcinogens. In *Air pollution and health*, Hester, R.E. and Harrison, R.M. (Eds.), The Royal Society of Chemistry, Cambridge, UK.

Li, C.T., Lin, Y.C., Lee, W.J. and Tsai, P.J. (2003). Emission of polycyclic aromatic hydrocarbons and their carcinogenic potencies from cooking sources to the urban atmosphere. *Environ. Health Perspect.* 111: 483.

Li, Y. and Delsante, A. (1996). Derivation of capture efficiency of kitchen range hoods in a confined space. *Build. Environ.* 31: 461–468.

Lunden, M.M., Delp, W.W. and Singer, B.C. (2015). Capture efficiency of cooking-related fine and ultrafine particles by residential exhaust hoods. *Indoor Air* 25: 45–58.

Malcolm, H. and Dobson, S. (1994). *The calculation of an environmental assessment level (EAL) for atmospheric PAHs using relative potencies,* Department of the Environment, London, UK.

McDonald, J.D., Zielinska, B., Fujita, E.M., Sagebiel, J.C., Chow, J.C. and Watson, J.G. (2003). Emissions from charbroiling and grilling of chicken and beef. *J. Air Waste Manage. Assoc.* 53: 185–194.

Mi, H.H., Liao, W.T., Chang, H.C., Chen, S.J., Lin, C.C. and Hsieh, L.T. (2014). Optical emission spectroscopy in cooking exhaust from a wet scrubber/atmospheric plasma reactor. *Aerosol Air Qual. Res.* 10: 1665–1674.

Nicas, M. (2006). The near field/far field (two-box) model with a constant contamination emission rate. In *Mathematical models for estimating occupational exposure to chemicals*. Keil, C.B., Simmons, C.E. and Anthony, T.R. (Eds.), American Industrial Hygiene Association (AIHA), Fairfax, VA, USA, pp. 47–52.

Nicas, M., Plisko, M.J. and Spencer, J.W. (2006). Estimating benzene exposure at a solvent parts washer. *J. Occup. Environ. Hyg.* 3: 284–291.

Nisbet, I.C. and LaGoy, P.K. (1992). Toxic equivalency factors (TEFs) for polycyclic aromatic hydrocarbons (PAHs). *Regul. Toxicol. Pharm.* 16: 290–300.

Reinke, P.H. and Keil, C.B. (2006). Well-mixed box model. In *Mathematical models for estimating occupational exposure to chemicals*, American Industrial Hygiene Association (AIHA), Fairfax, VA, USA, pp. 23–31.

Popiołek, Z., Trzeciakiewicz, Z. and Mierzwinski, S. (1998). Improvement of a plume volume flux calculation method. International conference on air distribution in rooms. Proceedings ROOMVENT '98, Stockhom, Sweden, Vol. 1, pp. 423–430.

Purcaro, G., Navas, J.A., Guardiola, F., Conte, L.S. and Moret, S. (2006). Polycyclic aromatic hydrocarbons in frying oils and snacks. *J. Food Protect.* 69: 199–204.

Rogge, W.F., Hildemann, L.M., Mazurek, M.A., Cass, G.R. and Simoneit, B.R. (1991). Sources of fine organic aerosol. 1. Charbroilers and meat cooking operations. *Environ. Sci. Technol.* 25: 1112–1125.

Saito, E., Tanaka, N., Miyazaki, A. and Tsuzaki, M. (2014). Concentration and particle size distribution of polycyclic aromatic hydrocarbons formed by thermal cooking. *Food Chem.* 153: 285–291.

Schauer, J.J., Kleeman, M.J., Cass, G.R. and Simoneit, B.R. (1999). Measurement of emissions from air pollution sources. 1. C_1 through C_{29} organic compounds from meat charbroiling. *Environ. Sci. Technol.* 33: 1566–1577.

Schauer, J.J., Kleeman, M.J., Cass, G.R. and Simoneit, B.R. (2002). Measurement of emissions from air pollution sources. 4. C_1-C_{27} organic compounds from cooking with seed oils. *Environ. Sci. Technol.* 36: 567–575.

See, S.W. and Balasubramanian, R. (2006). Physical characteristics of ultrafine particles emitted from different gas cooking methods. *Aerosol Air Qual. Res.* 6: 82–92.

See, S.W. and Balasubramanian, R. (2008). Chemical characteristics of fine particles emitted from different gas cooking methods. *Atmos. Environ.* 42: 8852–8862.

Siegmann, K. and Sattler, K. (1996). Aerosol from hot cooking oil, a possible health hazard. *J. Aerosol Sci.* 27: S493–S494.

Sjaastad, A.K., Jørgensen, R.B. and Svendsen, K. (2010). Exposure to polycyclic aromatic hydrocarbons (PAHs), mutagenic aldehydes and particulate matter during pan frying of beefsteak. *Occup. Environ. Med.* 67: 228–232.

Wang, G., Cheng, S., Wei, W., Wen, W., Wang, X. and Yao, S. (2015). Chemical characteristics of fine particles emitted from different chinese cooking styles. *Aerosol Air Qual. Res.* 15: 2357–2366.

Yik, F. and Au, P. (2002). Flow rate and capture efficiency of domestic kitchen exhaust hoods for chinese households. *Int. J. Archit. Sci.* 3: 125–134.

Zhang, S., Peng, S.C., Chen, T.H. and Wang, J.Z. (2015). Evaluation of inhalation exposure to carcinogenic PM_{10}-bound pahs of people at night markets of an urban area in a metropolis in eastern china. *Aerosol Air Qual. Res.* 15: 1944–1954.

Zhu, L.H. and Wang, J. (2003). Sources and patterns of polycyclic aromatic hydrocarbons pollution in kitchen air, China. *Chemosphere* 50: 611–618.